THE JOURNAL OF PHYSICAL CHEMISTRY B

Article

Formation of Ether-Functionalized Ionic Liquid-Based Aqueous Two-Phase Systems and Their Application in Separation of Protein and Saccharides

Zhijun Wang, Yuanchao Pei, Jing Zhao, Zhiyong Li, Yujuan Chen, and Kelei Zhuo

J. Phys. Chem. B, **Just Accepted Manuscript** • Publication Date (Web): 03 Mar 2015

Formation of Ether-Functionalized Ionic Liquid-Based Aqueous Two-Phase Systems and Their Application in Separation of Protein and Saccharides

Zhijun Wang, Yuanchao Pei, Jing Zhao, Zhiyong Li, Yujuan Chen, Kelei Zhuo*

Collaborative Innovation Center of Henan Province for Green Manufacturing of Fine Chemicals, Key Laboratory of Green Chemical Media and Reactions, Ministry of Education, School of Chemistry and Chemical Engineering, Henan Normal University, Xinxiang, Henan 453007, P. R. China, E-mail: klzhuo@263.net, Tel.: +86 373 3329056, Fax: +86-373-3329056

ABSTRACT

Ionic liquid (IL)-based aqueous two-phase systems (ATPSs) have attracted much attention in the separation technology. In this work, we synthesized five novel ether-functionalized ILs and studied their applications in ATPS formation. The phase diagrams for several systems were determined at 298.15 K. An as-prepared IL (1-(2-butoxy-ethyl)-3-methylimidazolium chloride) was chosen as a representative to construct ATPSs for separation of bovine serum albumin (BSA) from aqueous saccharide solutions. Results showed that 76.1% − 94.3% of BSA was enriched into the IL-rich top phase and almost all the saccharides were extracted into the salt-rich bottom phase in one-step separation process. The main factors affecting the separation process, such as kinds of saccharides and the amount of inorganic salts, were discussed. Furthermore, the size distributions of aggregates in the IL-rich top phase were determined by dynamic light scattering (DLS), and accordingly the possible mechanism for the separation was investigated.

KEYWORDS: aqueous two-phase system; ether-functionalized ionic liquid; bovine serum albumin; saccharides; separation

1. INTRODUCTION

Proteins and saccharides are important components of living organism, and coexist generally together. They are separated and purified difficultly. For example, the crude saccharides often contain a large number of non-carbohydrate substances, such as proteins.[1] Furthermore, the existence of saccharides causes significant deviation from the actual absorbance of proteins in the Bradford protein assay.[2] Therefore, the separation of the complex mixtures has become a focus of the researches. Several methods have been applied in the biological sample separation: gas chromatography/mass spectrometry, liquid-liquid extraction, and solid-phase extraction.[3,4] As a kind of liquid-liquid extractive technique, aqueous two-phase system (ATPS) is simple, low cost, and relatively reliable in scale-up, and has a great potential in separation application. Kula and co-workers published a number of papers describing the use of ATPS for protein purification.[5,6] The practical application of ATPSs to process development has been exploited for the recovery of biological products.[7-9]

Ionic liquids (ILs) as environment-friendly and designed solvents are attracting. In 2003, for the first time, Rogers and co-workers[10] reported on a new ATPS composed of a hydrophilic IL, 1-butyl-3-methylimidazolium chloride ($[C_4mim]Cl$), and a inorganic salt (K_3PO_4). The inorganic salt at a high concentration increased the hydrophobicity of the bottom phase containing rich-salt.[11] In rich-salt phase, the solubility of protein was markedly reduced because of the competition for water molecules between the protein and inorganic ions. Consequently, the addition of

inorganic salts enhances the transfer of protein from the bottom phase to the top phase.[12] Moreover, in the process of forming ATPSs, the negatively charged amino acids on the surface of protein interact with the positively charged IL-cation.[13] These factors promote the transfer of protein to the top phase. Therefore, we can change the structures of ILs and kinds of inorganic salts to improve the extraction efficiency of proteins using IL-based ATPSs. Recently, IL-based ATPSs are widely used for the separation and purification of various biomolecules,[14,15] based on their unique properties such as low viscosity, quick phase separation, high extraction efficiency, and gentle biocompatible environment.[16,17] A lot of researches were restricted to the extraction of the single component from one phase to another. However, IL-ATPS for separation of bovine serum albumin (BSA) from aqueous saccharide solutions was rarely reported. In previous work, we reported on the separation of BSA from aqueous saccharides solutions using an ATPS constructed by 1-butyl-3-methylimidazolium dicyanamide $[C_4mim][N(CN)_2]$, K_2HPO_4, and H_2O.[18] Results showed that more than 82% of BSA could be enriched into the IL-rich top phase and almost all the saccharides were extracted into the salt-rich bottom phase of ATPS. It is highly desired to construct new IL-based ATPSs for separations.

To form the IL-water biphasic systems for the extraction, hydrophobic ILs have to be used. Hydrophobic ILs are more expensive than hydrophilic ILs and the number of hydrophobic ILs is limited. In addition, using the simple IL-water biphasic systems for separation of biomacromolecules, their denaturation would happen possibly in the separation process.[18] Therefore, hydrophilic ILs are more likely used in the extraction

process. In recent decades, a lot of hydrophilic ILs were synthesized and applied to form ATPSs for extraction separation. For example, [C_6mim]Cl was used to construct ATPSs for extraction of BSA.[19] The ether-functionalized ILs also are hydrophilic. But compared with the alkyl-substituted ILs, they have a variety of unique properties, such as lower viscosity and lower melting point.[20-22] In addition, the ether group reduces the toxicity of ILs.[23] Therefore, it is significant to use the environment-friendly ether-based ILs for separation processes.

Herein, we synthesized five novel (except [C_2OC_2mim]Cl) hydrophilic ether-functionalized ionic liquids: 1-(2-alkoxy-ethyl)-3-methylimidazolium chloride ([$C_n OC_2$mim]Cl (n = 2, 3, 4)), 1-(2-propoxy-ethyl)-3-methylimidazolium p-toluenesulfonic acid ([C_3OC_2mim][p-TSA]), and 1-(2-benzyloxy-ethyl)-3-methylimidazolium p-toluenesulfonic acid ([PhCOC_2mim][p-TSA]). The ability of the ether-functionalized ILs for the formation of IL-based ATPSs was discussed. For such a purpose, phase diagrams for systems composed of different ether-functionalized ILs, inorganic salts (K_3PO_4/K_2HPO_4), and water at 298.15 K were determined. Then an as-prepared IL [C_4OC_2mim]Cl was used to form IL-based ATPSs for separating BSA from aqueous saccharide (glucose, sucrose, and dextran) solutions. Besides, dynamic light scattering (DLS) was applied to determine the size distribution of aggregates in the top IL-rich phase and to explore the possible mechanism for the separation of BSA.

2. EXPERIMENTAL SECTION

2.1 Materials. 1-Methylimidazole (CP) was purchased from HWRK Chemical Company (Beijing, China), 2-chloroethyl ethyl ether, 2-chloroethyl propyl ether, and 2-chloroethyl butyl ether were purchased from Tokyo Chemical Industry (TCI, Tokyo, Japan), respectively. They were used without further purification. Ethylene glycol propyl ether, p-toluenesulfonyl chloride, 4-dimethylaminopyridine, and 2-(benzyloxy) ethanol were purchased from Aladdin Chemistry (Los Angeles, USA). Triethylamine was purchased from Sinopharm Chemical Reagent Co (Shanghai, China). K_3PO_4 from TCI (Tokyo, Japan), K_2HPO_4 from Alfa Aesar (Ward Hill, MA, USA), bovine serum albumin (BSA), glucose, sucrose, and dextran (Mr~1500) from Sigma (St. Loius, MO, USA) were used without further purification. Ultrapure water was used to prepare solutions. All chemicals were of analytical grade.

2.2 Synthesis and Characterization of ILs. 1-(2-Alkoxy-ethyl)-3-methylimidazolium chlorides ($[C_nOC_2mim]Cl$ (n = 2, 3, 4)) were synthesized according to the procedure (Figure 1) described in the literature.[24] Chloroethyl alkylether was added dropwise to 1-methylimidazole under stirring at 0 °C. The reaction temperature increased to 80 °C. The mixture was stirred at 80 °C for 48 h, and then cooled to room temperature, washed three times with ethyl acetate. The ethyl acetate in produce was removed by rotary evaporation. The obtained ether-functionalized ILs products were dried under reduced pressure for 48 h at 50 °C in the presence of P_2O_5. The chemical structures of the ether-functionalized ILs were confirmed by ^{1}H NMR spectroscopy. Their ^{1}H NMR spectral characteristics were shown as follows:

$[C_2OC_2mim]Cl$: ^{1}H NMR (400 MHz, $CDCl_3$): δ 10.49 (*s*, 1H), 7.57 (*d*, 2H),

4.63-4.55 (*t*, 2H), 4.11 (*s*, 3H), 3.82-3.79 (*t*, 2H), 3.52 (*q*, 2H), 1.17 (*t*, 3H).

[C_3OC_2mim]Cl: ^{1}H NMR (400 MHz, $CDCl_3$): δ 10.49 (*s*, 1H), 7.47 (*s*, 1H), 7.46 (*s*, 1H), 4.57-4.53 (*t*, 2H), 4.06 (*s*, 3H), 3.77-3.71 (*t*, 2H), 3.36 (*t*, 2H), 1.51 (*q*, 2H), 0.82 (*t*, 3H).

[C_4OC_2mim]Cl: ^{1}H NMR (400 MHz, $CDCl_3$): δ 10.37 (*s*, 1H), 7.52 (*s*, 1H), 7.46 (*s*, 1H), 4.55-4.47 (*t*, 2H), 4.03 (*s*, 3H), 3.73-3.69 (*t*, 2H), 3.37 (*t*, 2H), 1.49 (*m*, 2H), 1.28-1.17 (*m*, 2H), 0.81 (*t*, 3H).

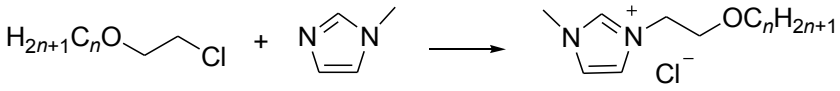

Figure 1. Synthesis process for [$C_nOC_2$mim]Cl (n = 2, 3, 4).

1-(2-Propoxy-ethyl)-3-methylimidazolium p-toluenesulfonic acid ([C_3OC_2mim][p-TSA]) and 1-(2-benzyloxy-ethyl)-3-methylimidazolium p-toluenesulfonic acid ([PhCOC_2mim][p-TSA]) were synthesized according to the procedure (Figures 2 and 3) described in the literature.[25,26] Ethylene glycol propyl ether was added to a dichloromethane solution of p-toluenesulfonyl chloride under stirring at 0 °C. Then triethylamine addition was followed by a catalytic amount of 4-dimethylaminopyridine. After 4 h the solution was washed with ultrapure water, brine, and sodium bicarbonate. After drying with sodium sulfate, dichloromethane was removed by rotary evaporation. Then p-toluenesulfonate was reacted with 1-methylimidazole under stirring at room temperature. After 48 h the mixture was washed three times with ethyl acetate. The ethyl acetate was removed by rotary evaporation. The synthesis of ionic liquid [PhCOC_2mim][p-TSA] followed the same procedure as the preparation of [C_3OC_2mim][p-TSA]. The obtained

ether-functionalized ILs products were dried under reduced pressure for 48 h at 50 °C in the presence of P_2O_5. Their ^1H NMR spectral characteristics were shown as follows:

[C_3OC_2mim][p-TSA]: ^1H NMR (400 MHz, $CDCl_3$): δ 9.61 (*s*, 1H), 7.73 (*s*, 1H), 7.71 (*s*, 1H), 7.37 (*m*, 2H), 7.11 (*d*, 2H), 4.37-4.34 (*t*, 2H), 3.88 (*s*, 3H), 3.65-3.61 (*t*, 2H), 3.30 (*t*, 2H), 2.30 (*s*, 3H), 1.52-1.43 (*m*, 2H), 0.80 (*t*, 3H).

[$PhCOC_2$mim][p-TSA]: ^1H NMR (400 MHz, $CDCl_3$): δ 9.69 (*s*, 1H), 7.76 (*s*, 1H), 7.74 (*s*, 1H), 7.32-7.25 (*m*, 5H), 7.22-7.19 (*m*, 2H), 7.11 (*d*, 2H), 4.47-4.39 (*m*, 4H), 3.90 (*s*, 3H), 3.74 (*t*, 2H), 2.31 (*s*, 3H).

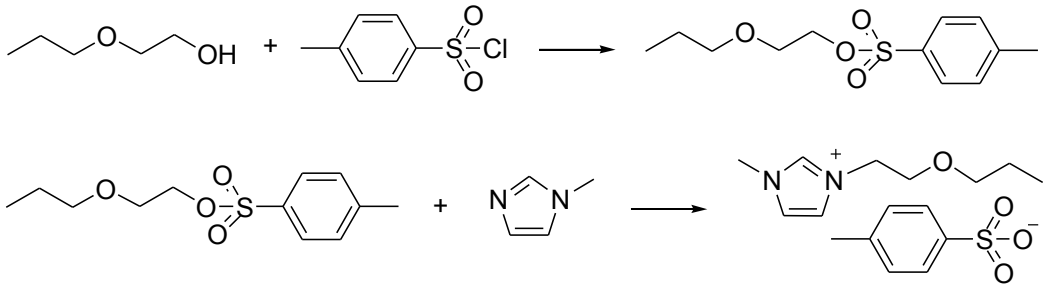

Figure 2. Synthesis process for [C_3OC_2mim][p-TSA].

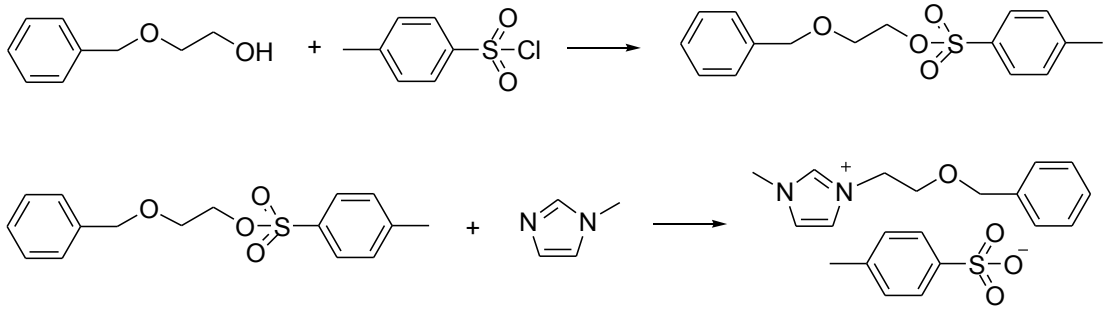

Figure 3. Synthesis process for [$PhCOC_2$mim][p-TSA].

At the same time, based on the graphs of thermogravimetric analysis (TGA) and differential scanning calorimetry (DSC), the thermal decomposition temperature and glass transition temperature were obtained, and are given in Table 1. Both

measurements were carried out under N_2 with a temperature ramp of 10 K/min.

Table 1. Melting Point (T_m) and Thermal Decomposition Temperature (T_d) of ILs.

Ionic liquid	T_m/°C	T_d/°C
$[C_3OC_2mim][p\text{-}TSA]$	50.79	336.0
$[PhCOC_2mim][p\text{-}TSA]$	−23.87[a]	328.8
$[C_2OC_2mim]Cl$	–35.98[a]	257.8
$[C_3OC_2mim]Cl$	−40.66[a]	257.0
$[C_4OC_2mim]Cl$	–45.95[a]	254.3

[a] glass transition temperature

2.3 Preparation of Phase Diagrams. The phase diagrams were determined by the turbid titration method.[10,18] In short, a few grams of ether-based IL were weighed into a test tube. Then a small amount of water was added to the tube for dissolving the IL. A known-concentration solution of salt was added dropwise to the test tube until the mixture became turbid. The added volume of the salt solution was recorded and the composition of this mixture was calculated. Then a few drops of water was added to make the two-phase system clear again. The above procedure was repeated to gain enough data for constructing a liquid-liquid equilibrium binodal curve. The concentration of the phase components was determined by weight quantification of all the components with a standard uncertainty of 10^{-4} g. The tie lines, which depict the concentrations of IL and salt in the top/bottom phases, were determined with the process outlined in our previous work.[27]

2.4 Separation of Protein from Saccharides. Method for the separation of protein

from saccharides is similar to our previous work.[18,28] The details are given in the Supporting Information. The dynamic light scattering (DLS) measurements were carried out using Zeta-Meter (Nano-ZS 90) laser light scattering photometer (Malvern, U.K.).[18] Also see the Supporting Information.

3. RESULTS AND DISCUSSION

3.1 Phase Diagram of IL-Based ATPS. The binodal curves and tie lines for the ether-functionalized IL + salt systems were determined at 298.15 K, and shown in Figures 4–6 and Figures S1–S3 in the Supporting Information, respectively.

The binodal data were correlated by the following equation:[29]

$$w_1 = a\ln(w_2 + c) + b \quad (3)$$

where w_1 and w_2 are the mass fractions of ILs and salts, respectively, and a, b, and c, are fitting parameters. The fitting parameters gained from the correlation of experimental binodal data are given in Table 2, along with the correlation coefficients (R^2) and the corresponding standard deviations (s) of eq 3. Based on the obtained R^2 and s, we can conclude that eq 3 has more satisfactory accuracy in binodal data fitting for the studied systems.[29]

Table 2. Parameters (a, b, and c) Obtained by the Regression of the Experimental Binodal Data Through the Application of Eq 3 for the IL(1) + Salt(2) + H_2O Systems at 298.15 K.

systems	a	b	c	R^2	$10^3 s$
$[C_2OC_2mim]Cl + K_3PO_4 + H_2O$	−0.31488	−0.22952	0.09645	0.9987	2.1
$[C_2OC_2mim]Cl + K_2HPO_4 + H_2O$	−0.20134	−0.18407	−0.02090	0.9975	1.3

$[C_3OC_2mim]Cl + K_3PO_4 + H_2O$	−0.22889	−0.20371	0.02362	0.9995	1.8
$[C_3OC_2mim]Cl + K_2HPO_4 + H_2O$	−0.20764	−0.20321	−0.02012	0.9954	1.3
$[C_3OC_2mim][p\text{-}TSA] + K_3PO_4 + H_2O$	−0.37854	−0.51823	0.03649	0.9961	4.0
$[C_4OC_2mim]Cl + K_3PO_4 + H_2O$	−0.29155	−0.20758	0.11986	0.9997	1.1
$[C_4OC_2mim]Cl + K_2HPO_4 + H_2O$	−0.25214	−0.21485	−0.03914	0.9985	2.2
$[PhCOC_2mim][p\text{-}TSA] + K_3PO_4 + H_2O$	−0.12733	−0.27418	−0.04208	0.9930	1.8

3.1.1 Effect of the structure of ILs. ILs composed of different cations and anions have different hydrophobicity. ATPSs can be constructed by adding a certain amount of K_2HPO_4 or K_3PO_4 to aqueous IL solutions. Figure 4 indicates the influence of the alkyl-chain length of ILs on the phase diagrams. Obviously, the phase-forming ability of these ILs is observed: $[C_4OC_2mim]Cl$ > $[C_3OC_2mim]Cl$ > $[C_2OC_2mim]Cl$. This order is in agreement with chaotropic ability of IL-cations. The difference in chaotropic ability results from the structural difference of the cations.[30] With the increase of the alkyl-chain length ($[C_nOC_2mim]^+$ (n = 2, 3, 4)), the binodal curves are more closer to the origin,[31] showing that the phase-forming ability of ILs increases with increasing alkyl-chain length. That is to say, $[C_4OC_2mim]Cl$ is the most chaotropic salt and this binodal is furthest to the left (it is the easiest to salt-out). Obviously, the phase-forming ability of $[C_4OC_2mim]Cl$ is the best among the three ILs.

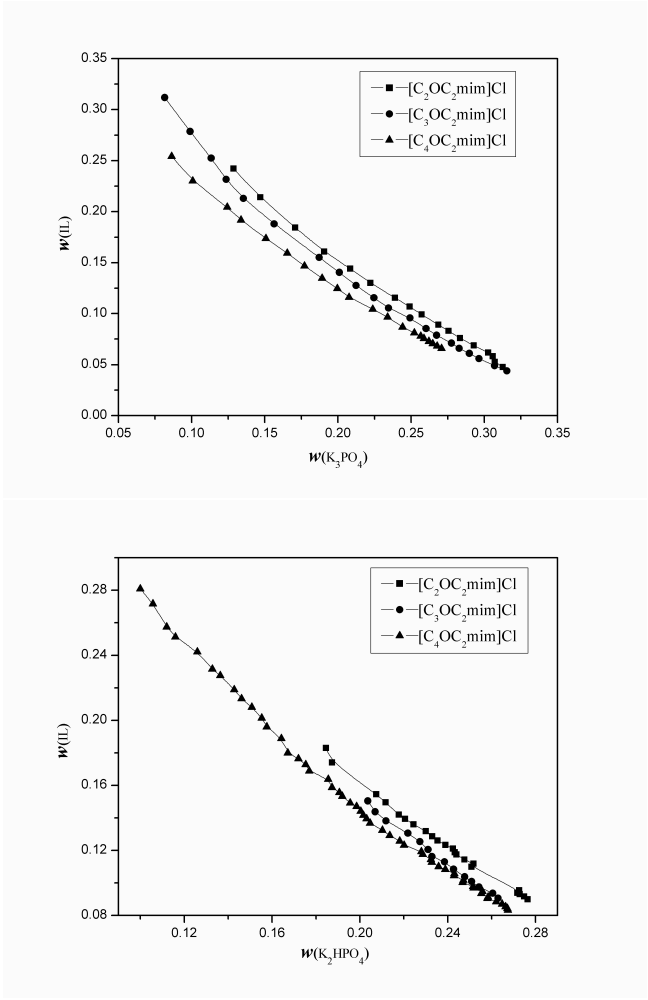

Figure 4. Phase diagrams for the aqueous two-phase systems composed by $[C_2OC_2mim]Cl$ / $[C_3OC_2mim]Cl$ / $[C_4OC_2mim]Cl$ + K_3PO_4 / K_2HPO_4 at 298.15 K: *w*, mass fraction.

Figure 5 indicates the effect of ions of ether-based ILs on the phase diagram. At a certain amount of K_3PO_4, the phase-forming ability of these ILs is observed: $[PhCOC_2mim][p\text{-}TSA]$ > $[C_3OC_2mim][p\text{-}TSA]$ > $[C_3OC_2mim]Cl$. This can be interpreted by the facts that the addition of the electro-rich aromatic π system (hydrophobic) to the cation and anion increases the hydrophobicity of the IL,[32,33] and then increase the phase-forming ability. Therefore, we suggest that the hydrophobicity of the ILs play a critical role in aqueous two-phase extraction process.

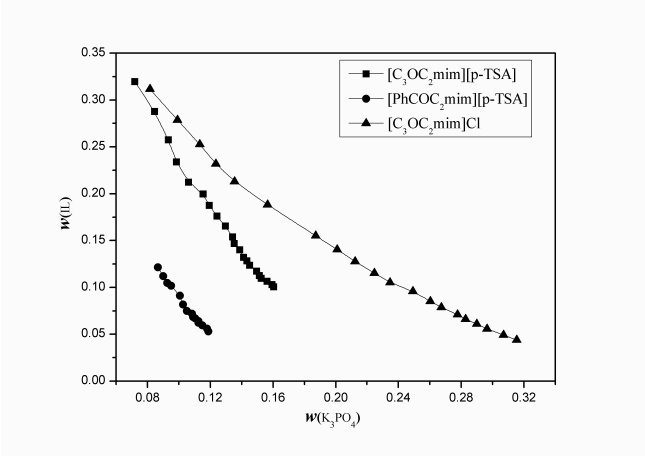

Figure 5. Phase diagrams for the aqueous two-phase systems composed by [$PhCOC_2$mim][p-TSA] / [C_3OC_2mim][p-TSA] / [C_3OC_2mim]Cl + K_3PO_4 at 298.15 K: *w*, mass fraction.

3.1.2 Effect of salt category. Figure 6 shows the phase diagrams for the ATPSs of [C_4OC_2mim]Cl with K_2HPO_4/K_3PO_4. It can be seen that the binodal curve for K_3PO_4 is closer to the origin than that for K_2HPO_4. Consequently, the phase-forming ability of both salts is: K_3PO_4 > K_2HPO_4. This order is the same as the previous researches on the ATPSs of [C_4min]X (X=Cl or Br) and [$C_n$min]Br (*n* = 6 or 8).[30,34] Since cation of both salts is the same K^+, but anions are different, the phase-forming ability is controlled by different anions. Results showed that anion with higher valence was used for constructing ATPSs, a lower concentration of salt was needed. It may be explained by their different salting-out abilities (kosmotropicity): the higher valent anions show bigger salting-out ability, because the anions with high charge density can hydrate more water molecules, and thus the less water is available to hydrate ILs. This is identical to the hydration Gibbs free energy of the anions: HPO_4^{2-} (−1125 kJ·mol^{-1}), PO_4^{3-} (–2765 kJ·mol^{-1}).[35] The order is also in agreement with the strength of the kosmotropic salts (Hofmeister series). Since K_2HPO_4 is able to make a suitable

pH range for the gentle separation of BSA, it was selected for the further researches in the present work.

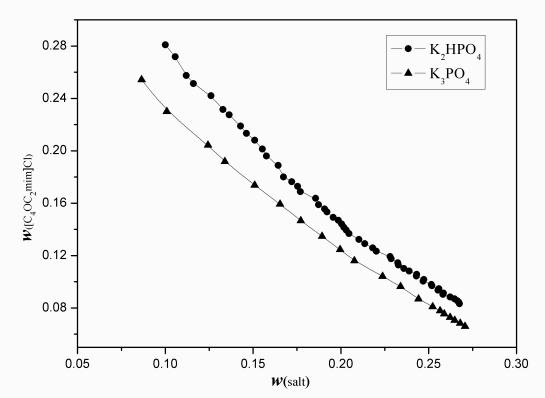

Figure 6. Phase diagrams for the aqueous two-phase systems composed by $[C_4OC_2mim]Cl$+ K_3PO_4 / K_2HPO_4 at 298.15 K: *w*, mass fraction.

3.2 Separation of BSA and Saccharides in $[C_4OC_2mim]Cl + K_2HPO_4$ ATPSs

3.2.1 Effect of inorganic salt amount. Amount of salts is a key factor to control the extraction efficiency.[36] As shown in Figure 7, as the concentration of salts (K_2HPO_4) increases, the extraction yield for BSA increases at first and decreases afterwards. The possible reason is that K_2HPO_4 has a strong salting-out effect.[37] When kosmotropic ions were added into aqueous solutions of ILs, the molecules of water surrounding the ions would become electro-constriction states. Hence, the hydrogen bonding of water was increased in the phase, and thus more energy is required to form a cavity in this solution for the organic cation $[C_4OC_2mim]^+$.[10] As the concentration of salt increases, the salt-rich bottom phase became more hydrophobic[38] and more structured, and consequently the solubility of protein was markedly reduced because of the competition for water molecules between the protein molecules and inorganic ions.[12]

Moreover, in the process of forming ATPSs, the negatively charged amino acids on the surface of protein interact with the positively charged IL-cation.[13] These factors lead to a larger transfer of protein to the top IL-rich phase. At a given content of inorganic salt, the ILs with the more hydrophobic cations and the less water-structuring anions would be separated from the inorganic salts. However, extraction efficiency decreases when the content of inorganic salt is too high. The possible reason is the denaturation of protein to some extent under the circumstance. Furthermore, thes ch hydrophilic ILs from water soluti ppropriate for the extraction of biom

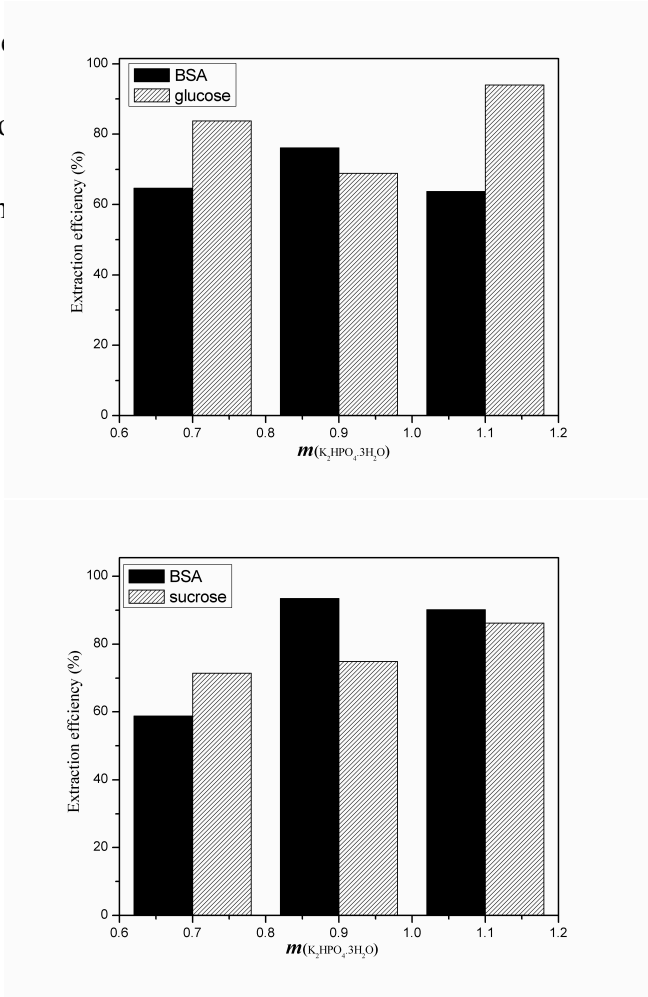

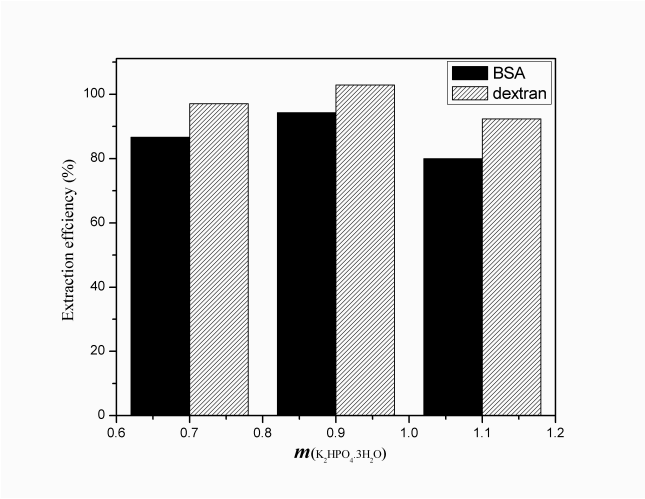

Figure 7. Effect of the concentration of salt on the extraction efficiency of BSA and saccharides in $[C_4OC_2mim]Cl$ + $K_2HPO_4{\cdot}3H_2O$ ATPSs at 298.15 K: the concentrations of BSA and saccharides were at 4.0 $mg{\cdot}mL^{-1}$ and 1.0 $mg{\cdot}mL^{-1}$, respectively; 0.4 g IL, 1.2 mL H_2O were added for the construction of ATPSs; *m* (g) is the total mass of $K_2HPO_4{\cdot}3H_2O$ added. The deviations of extraction efficiency of BSA and saccharides were 2% and 5%, respectively.

3.2.2 Effect of different saccharides. Table 3 shows that the extraction yields of different saccharides and BSA in $[C_4OC_2mim]Cl$ + K_2HPO_4 ATPSs. From this table, we observed that the extraction yields for BSA from the saccharide solutions increase with the increase of the number of hydroxyl groups in a saccharide molecule (dextran > sucrose > glucose). The extraction yields of BSA from different saccharide solutions are different. Most of the sugars were separated into the salt-rich phase. Because of the positive values of viscosity *B* coefficients of saccharides in aqueous solutions, the saccharide molecules act overall as kosmotropes (to form stronger hydrogen bond networks with water).[39,41,42] Moreover, the greater the number of hydroxyl groups on a sugar molecule, the more kosmotropic the sugar. Therefore, the presence of sugar in the $[C_4OC_2mim]Cl$ + K_2HPO_4 ATPS would be benefited to the

separation of kosmotropic salt K_2HPO_4. Because of the formation of hydrogen bonds between water and saccharide molecules, the content of free water in the bottom salt-rich phase will decrease, which forces more chaotropic IL and BSA to be transferred into the top IL-rich phase, compared with the ATPSs without saccharides. Consequently, the number of hydroxyl groups on saccharide molecules is a key factor influencing the distribution of saccharides and BSA in these ATPSs.

Experimental results showed that 76.1% − 94.3% of the BSA were extracted into the top IL-rich phase and sugars were separated into the bottom salt-rich phase in one-step separation process. Compared with our previous work,[18] the ATPSs based on ether-functionalized ILs also exhibit excellent extraction efficiency for BSA from aqueous saccharides. Furthermore, the ether-based ILs possess low viscosity, low melting point, and low toxicity, and thus have wide application in the extraction separation by using IL-based ATPSs.

Table 3. Extraction efficiencies (E) of BSA and saccharides in $[C_4OC_2mim]Cl + K_2HPO_4$ ATPSs at 298.15 K[a]

Saccharide	E_{BSA}%	$E_{saccharide}$%
glucose	76.1	68.9
sucrose	93.5	74.9
dextran	94.3	102.9

[a] Test concentrations of BSA and saccharides were at 4.0 mg·mL^{-1} and 1.0 mg·mL^{-1}, respectively; 0.4 g of IL, 0.9 g of $K_2HPO_4 \cdot 3H_2O$, and 1.2 mL of H_2O were mixed for the construction of ATPSs.

3.3 Size Distribution of Aggregates. In order to understand the separation process, we measured the size distribution of aggregates in the IL-ATPSs. In the $[C_4OC_2mim]Cl + K_2HPO_4$ ATPS, the IL-rich top phase consists of IL, less amount of inorganic salt, and water, and the salt-rich bottom phase consists of inorganic salt, less amount of IL, and water. In the top IL-rich phase, the presence of high IL concentration causes a remarkable aggregation of cations of the IL due to their amphiphilic characteristics.[43] To confirm the state of $[C_4OC_2mim]Cl$ in the IL-rich phase, we measured the size distribution of aggregates for $[C_4OC_2mim]Cl$ and BSA in the aqueous solution by DLS at 298.15 K, and the results are shown in Figure 8. Obviously, when BSA was added to the ATPS, a novel aggregate was generated at 260 nm. The novel aggregate is larger than both BSA and IL aggregates. The similar results were obser Ve could conclude that the separatio f novel IL-protein complex aggregat

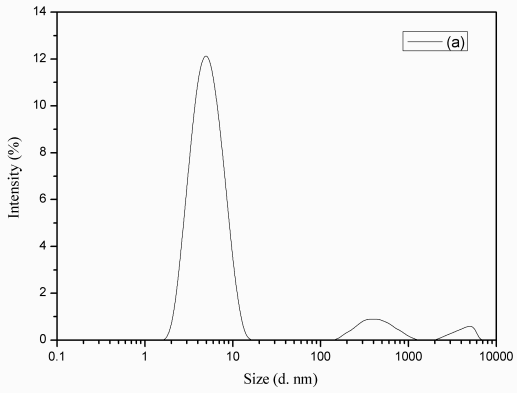

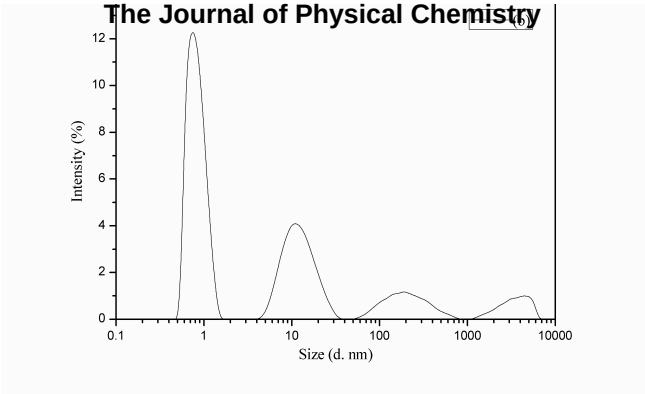

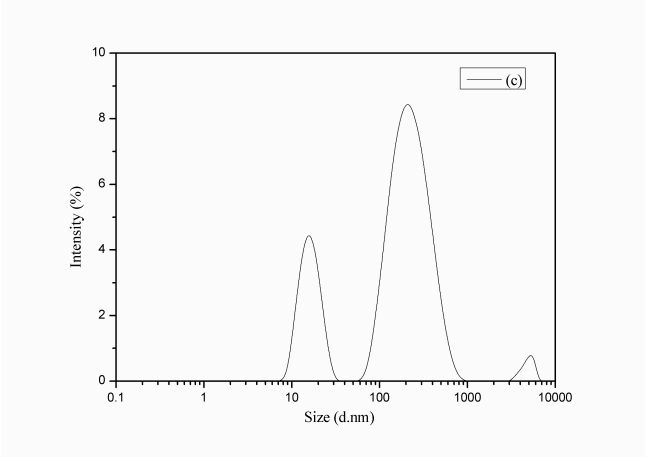

Figure 8. Size distribution of the aggregates of BSA, IL, and BSA + IL in aqueous solution: (a) BSA (1.23 $g \cdot L^{-1}$); (b) IL (1.2 $mol \cdot kg^{-1}$); (c) BSA (1.23 $g \cdot L^{-1}$) + IL (1.2 $mol \cdot kg^{-1}$).

4. CONCLUSIONS

In this work, we synthesized five novel hydrophilic ether-functionalized ionic liquids and studied their applications in ATPS formation. The phase diagrams for several systems were determined at 298.15 K. The results showed that BSA was extracted into the IL-rich top phase but most of saccharides were transferred into the salt-rich bottom phase. Extraction yield of BSA enhanced with increasing the number of hydroxyl groups in a saccharide molecule (dextran > sucrose > glucose). The generation of the novel IL-protein complex aggregates is a key factor for separation of BSA from the aqueous solutions of saccharides. We expect that $[C_4OC_2mim]Cl$ +

K_2HPO_4 ATPSs have a potential to separate protein from saccharide solutions, and therefore highlight a new opportunity of ether-functionalized IL-ATPSs to separate biomolecules from complex systems.

ASSOCIATED CONTENT

Supporting Information

Experiments for preparation of phase diagrams, separation of protein from saccharides, and dynamic light scattering measurements; Phase diagrams for $[C_nOC_2mim]Cl$ (n = 2, 3, 4) + K_2HPO_4 aqueous two-phase systems at 298.15 K; binodal data for the ether-functionalized ILs (1) + K_3PO_4 / K_2HPO_4 (2) + H_2O (3) ATPSs at T = 298.15 K.

AUTHOR INFORMATION

Corresponding Author

*Tel: +86-373-3329056; fax: +86-373-3329056; e-mail: klzhuo@263.net

Notes

The authors declare no competing financial interest.

ACKNOWLEDGMENTS

Financial supports from the National Natural Science Foundation of China (Nos. 21173070，21303044) and the Plan for Scientific Innovation Talent of Henan Province (No. 124200510014) are gratefully acknowledged.

REFERENCES

(1) Wu, Y.; Cui, S. W.; Tang, J.; Gu, X. Optimization of Extraction Process of Crude Polysaccharides from Boat-Fruited Sterculia Seeds by Response Surface Methodology. *Food Chem.*

2007, *105*, 1599–1605.

(2) Banik, S. P.; Pal, S.; Ghorai, S.; Chowdhury, S.; Khowala, S. Interference of Sugars in the Coomassie Blue G Dye Binding Assay of Proteins. *Anal. Biochem.* **2009**, *386*, 113–115.

(3) Catlin, D.; Kammerer, R. C.; Hatton, C.; Sekera, M.; Merdink, J. Analytical Chemistry at the Games of the XXIIIrd Olympiad in Los Angeles, 1984. *Clin. Chem.* **1987**, *33*, 319–327.

(4) Leinonen, A.; Kuuranne, T.; Kostiainen, R. Liquid Chromatography/Mass Spectrometry in Anabolic Steroid Analysis—Optimization and Comparison of Three Ionization Techniques: Electrospray Ionization, Atmospheric Pressure Chemical Ionization and Atmospheric Pressure Photoionization. *J. Mass. Spectrom.* **2002**, *37*, 693–698.

(5) Frerix, A.; Schönewald, M.; Geilenkirchen, P.; Müller, M.; Kula, M.-R.; Hubbuch, J. Exploitation of the Coil-globule Plasmid DNA Transition Induced by Small Changes in Temperature, pH Salt, and Poly (Ethylene Glycol) Compositions for Directed Partitioning in Aqueous Two-Phase Systems. *Langmuir* **2006**, *22*, 4282–4290.

(6) Ruther, T.; Harris, K. R.; Horne, M. D.; Kanakubo, M.; Rodopoulos, T.; Veder, J. P.; Woolf, L. A. Transport, Electrochemical and Thermophysical Properties of Two N-Donor-Functionalised Ionic Liquids. *Chem. Eur. J.* **2013**, *19*, 17733–17744.

(7) Benavides, J.; Rito-Palomares, M. Practical Experiences from the Development of Aqueous Two-Phase Processes for the Recovery of High Value Biological Products. *J. Chem. Technol. Biotechnol.* **2008**, *83*, 133–142.

(8) Flieger, J.; Czajkowska-Żelazko, A. *Applications of Ionic Liquids in Science and Technology*; InTech, Vienna, Austria, 2011, 311–342.

(9) Flieger, J.; Czajkowska-Żelazko, A. Aqueous Two Phase System Based on Ionic Liquid for Isolation of Quinine from Human Plasma Sample. *Food Chem.* **2015**, *166*, 150–157.

(10) Gutowski, K. E.; Broker, G. A.; Willauer, H. D.; Huddleston, J. G.; Swatloski, R. P.; Holbrey, J. D.; Rogers, R. D. Controlling the Aqueous Miscibility of Ionic Liquids: Aqueous Biphasic Systems of Water-Miscible Ionic Liquids and Water-Structuring Salts for Recycle, Metathesis, and Separations. *J. Amer. Chem. Soc.* **2003**, *125*, 6632–6633.

(11) Zasllavsky, B.Y.; Miheeva, L.M.; Mesteckina, N.M.; Rogozhin, S.V. Physicochemical Factors Governing Partition Behaviour of Solutes and Particles in Aqueous Polymeric Biphasic Systems. II. Effect of Ionic Composition on the Hydration Properties of the Phases. *J. Chromatogr. A* **1982**, *253*, 149–158.

(12) Pei, Y. C.; Wang, J. J.; Wu, K.; Xuan, X. P.; Lu, X. J. Ionic Liquid-Based Aqueous Two-Phase Extraction of Selected Proteins. *Sep. Purif. Technol.* **2009**, *64*, 288–295.

(13) Dreyer, S.; Salim, P.; Kragl, U. Driving Forces of Protein Partitioning in an Ionic Liquid-Based Aqueous Two-Phase System. *Biochem. Eng. J.* **2009**, *46*, 176–185.

(14) Novak, U.; Pohar, A.; Plazl, I.; Znidarsic-Plazl, P. Ionic Liquid-Based Aqueous Two-Phase Extraction within a Microchannel System. *Sep. Purif. Technol.* **2012**, *97*, 172–178.

(15) Ventura, S. P. M.; Sousa, S. G.; Serafim, L. S.; Lima, A. S.; Freire, M. G.; Coutinho, J. A. P. Ionic Liquid-Based Aqueous Biphasic Systems with Controlled pH: The Ionic Liquid Anion Effect. *J. Chem. Eng. Data* **2012**, *57*, 507–512.

(16) Azevedo, A. M.; Gomes, A. G.; Rosa, P. A.; Ferreira, I. F.; Pisco, A. M.; Aires-Barros, M. R. Partitioning of Human Antibodies in Polyethylene Glycol–Sodium Citrate Aqueous Two-Phase Systems. *Sep. Purif. Technol.* **2009**, *65*, 14–21.

(17) Azevedo, A. M.; Rosa, P. A.; Ferreira, I. F.; Aires-Barros, M. R. Chromatography-Free Recovery of Biopharmaceuticals through Aqueous Two-Phase Processing. *Trends biotechnol.* **2009**, *27*,

240–247.

(18) Pei, Y. C.; Li, Z. Y.; Liu, L.; Wang, J. J.; Wang, H. Y. Selective Separation of Protein and Saccharides by Ionic Liquids Aqueous Two-Phase Systems. *Sci. China. Chem.* **2010**, *53*, 1554–1560.

(19) Regupathi, I; Monteiro, S. L. 1-Hexyl-3-Methylimidazolium Chloride-Potassium Carbonate Aqueous Two Phase System: Equilibrium Characteristics and BSA Partitioning Behavior. *J. Dispersion Sci. Technol.* **2014**, *35*, 418–427.

(20) Fang, S.; Jin, Y.; Yang, L.; Hirano, S.-i.; Tachibana, K.; Katayama, S. Functionalized Ionic Liquids Based on Quaternary Ammonium Cations with Three or Four Ether Groups as New Electrolytes for Lithium Battery. *Electrochim. Acta* **2011**, *56*, 4663–4671.

(21) Kakibe, T.; Yoshimoto, N.; Egashira, M.; Morita, M. Optimization of Cation Structure of Imidazolium-Based Ionic Liquids as Ionic Solvents for Rechargeable Magnesium Batteries. *Electrochem. Commun.* **2010**, *12*, 1630–1633.

(22) Monteiro, M. J.; Camilo, F. F.; Ribeiro, M. C.; Torresi, R. M. Ether-Bond-Containing Ionic Liquids and the Relevance of the Ether Bond Position to Transport Properties. *J. Phys. Chem. B* **2010**, *114*, 12488–12494.

(23) Tang, S.; Baker, G. A.; Zhao, H. Ether-and Alcohol-Functionalized Task-Specific Ionic Liquids: Attractive Properties and Applications. *Chem. Soc. Rev.* **2012**, *41*, 4030–4066.

(24) Liu, Q.; Janssen, M. H.; van Rantwijk, F.; Sheldon, R. A. Room-Temperature Ionic Liquids that Dissolve Carbohydrates in High Concentrations. *Green Chem.* **2005**, *7*, 39–42.

(25) Dzyuba, S. V.; Bartsch, R. A. New Room-Temperature Ionic Liquids with C_2-Symmetrical Imidazolium Cations. *Chem. Commun.* **2001**, (16), 1466–1467.

(26) Sammelson, R. E.; Casida, J. E. Synthesis of a Tritium-Labeled, Fipronil-Based, Highly Potent, Photoaffinity Probe for the GABA Receptor. *J. Org. Chem.* **2003**, *68*, 8075–8079.

(27) Pei, Y. C.; Wang, J. J.; Liu, L.; Wu, K.; Zhao, Y. Liquid-Liquid Equilibria of Aqueous Biphasic Systems Containing Selected Imidazolium Ionic Liquids and Salts. *J. Chem. Eng. Data* **2007**, *52*, 2026–2031.

(28) Dubois, M.; Gilles, K. A.; Hamilton, J. K.; Rebers, P. t.; Smith, F. Colorimetric Method for Determination of Sugars and Related Substances. *Anal. Chem.* **1956**, *28*, 350–356.

(29) Han, J.; Wang, Y.; Li, Y.; Yu, C.; Yan, Y. Equilibrium Phase Behavior of Aqueous Two-Phase Systems Containing 1-Alkyl-3-methylimidazolium Tetrafluoroborate and Ammonium Tartrate at Different Temperatures: Experimental Determination and Correlation. *J. Chem. Eng. Data* **2011**, 56, 3679–3687.

(30) Bridges, N. J.; Gutowski, K. E.; Rogers, R. D. Investigation of Aqueous Biphasic Systems formed from Solutions of Chaotropic Salts with Kosmotropic Salts (Salt–Salt ABS). *Green Chem.* **2007**, *9*, 177–183.

(31) Pal, A.; Chaudhary, S. Ionic Liquid Induced Alterations in the Physicochemical Properties of Aqueous Solutions of Sodium Dodecylsulfate (SDS). *Colloids Surf., A* **2013**, *430*, 58–64.

(32) Pei, Y. C.; Wang, J. J.; Xuan, X. P.; Fan, J.; Fan, M. Factors Affecting Ionic Liquids Based Removal of Anionic Dyes from Water. *Environ. Sci. Technol*. **2007**, *41* (14), 5090–5095.

(33) Hassan, S.; Duclaux, L.; Lévêque, J. M.; Reinert, L.; Farooq, A.; Yasin, T. Effect of Cation Type, Alkyl Chain Length, Adsorbate Size on Adsorption Kinetics and Isotherms of Bromide Ionic Liquids from Aqueous Solutions onto Microporous Fabric and Granulated Activated Carbons. *J. Environ. Manage.* **2014**, *144* (0), 108–117.

(34) Pei, Y. C.; Wang, J. J.; Liu, L.; Wu, K.; Zhao, Y. Liquid-Liquid Equilibria of Aqueous Biphasic Systems Containing Selected Imidazolium Ionic Liquids and Salts. *J. Chem. Eng. Data* **2007**, *52*,

2026–2031.

(35) Marcus, Y. Thermodynamics of Solvation of Ions. Part 5.—Gibbs Free Energy of Hydration at 298.15 K. *J. Chem. Soc., Faraday Trans.* **1991**, *87*, 2995–2999.

(36) Trindade, J. R.; Visak, Z. P.; Blesic, M.; Marrucho, I. M.; Coutinho, J. A. P.; Lopes, J. N. C.; Rebelo, L. P. N. Salting-Out Effects in Aqueous Ionic Liquid Solutions: Cloud-Point Temperature Shifts. *J. Phys. Chem. B* **2007**, *111*, 4737–4741.

(37) Arakawa, T.; Timasheff, S. N. Preferential Interactions of Proteins with Salts in Concentrated Solutions. *Biochem.* **1982**, *21*, 6545–6552.

(38) Louros, C. L.; Cláudio, A. F. M.; Neves, C. M.; Freire, M. G.; Marrucho, I. M.; Pauly, J.; Coutinho, J. A. Extraction of Biomolecules Using Phosphonium-Based Ionic Liquids + K_3PO_4 Aqueous Biphasic Systems. *Int. J. Mol. Sci.* **2010**, *11*, 1777–1791.

(39) Wu, B.; Zhang, Y.; Wang, H. Phase Behavior for Ternary Systems Composed of Ionic Liquid+ Saccharides+ Water. *J. Phys. Chem. B* **2008**, *112*, 6426–6429.

(40) Wu, B.; Zhang, Y. M.; Wang, H. P. Aqueous Biphasic Systems of Hydrophilic Ionic Liquids+ Sucrose for Separation. *J. Chem. Eng. Data* **2008**, *53*, 983–985.

(41) Mathpal, R.; Joshi, B. K.; Joshi, S.; Kandpal, N. D. Intermolecular Forces of Sugars in Water. *Monatsh. Chem. - Chem. Mon.* **2006**, *137*, 375–379.

(42) Zhao, H. Are Ionic Liquids Kosmotropic or Chaotropic? An Evaluation of Available Thermodynamic Parameters for Quantifying the Ion Kosmotropicity of Ionic Liquids. *J. Chem. Technol. Biotechnol.* **2006**, *81*, 877–891.

(43) Wang, H.; Wang, J.; Zhang, S.; Xuan, X. Structural Effects of Anions and Cations on the Aggregation Behavior of Ionic Liquids in Aqueous Solutions. *J. Phys. Chem. B* **2008**, *112*,

16682–16689.

(44) Aivaliotis, M.; Samolis, P.; Neofotistou, E.; Remigy, H.; Rizos, A. K.; Tsiotis, G. Molecular Size Determination of a Membrane Protein in Surfactants by Light Scattering. *Biochim. Biophys. Acta - Biomembranes* **2003**, *1615*, 69–76.

(45) Spelzini, D.; Peleteiro, J.; Picó, G.; Farruggia, B. Polyethyleneglycol–Pepsin Interaction and Its Relationship with Protein Partitioning in Aqueous Two-Phase Systems. *Colloids Surf., B* **2008**, *67*, 151–156.

A Table of Contents Image